

Jet simulation in a diesel engine

James Glimm^{a,b}, M.N. Kim^b, X.-L. Li^a, R. Samulyak^b, Z.-L. Xu^{b,*}

^a Department of Applied Mathematics and Statistics, University at Stony Brook, Stony Brook, NY 11794, USA

^b Center for Data Intensive Computing, Brookhaven National Laboratory, Upton, NY 11793, USA

Abstract

In this paper, we report a numerical study of the jet breakup and spray formation in a diesel engine by the Front Tracking method. We model a mixed vapor–liquid region through a heterogeneous model with dynamic vapor bubble insertion. On the liquid/vapor interface, a phase transition problem is solved numerically.

Keywords: Jet stimulation; Front Tracking method; Diesel engine

1. Introduction

The mechanisms of jet breakup and spray formation of a high-speed diesel jet injected through a circular nozzle are the key to design a fuel efficient, nonpolluting diesel engine. Many parameters such as the nuzzle shape, the velocity and the turbulence of the jet and the thermodynamic states of liquid and gas could be contributing causes for jet breakup. Our goal is to model the spray at a micro-physical level, with the creation of individual droplets. We conduct the simulations for the jet breakup within a 2D axis-symmetric geometry.

In our previous study [1], we have used the homogeneous EOS model to describe the jet flow including the mixed liquid-vapor region. The diesel fuel is treated as isentropic with a piecewise analytic EOS $P = P(\rho)$. We have found that since the flow in the jet leaving the nozzle is too fast and the breakup is too rapid for Kelvin-Helmholtz instabilities to be the primary driving force for the breakup at the jet surface. We conclude that there are other significant events in the nozzle flow upstream of the jet to provide the breakup mechanism. The flow is at high Reynolds number, but we have also concluded that the pure liquid flow is laminar, i.e. non-turbulent, under experimental conditions due to the short length of the nozzle.

We have also observed the formation of the cavitation in the flow, which indicates the vaporization of the liquid. We then study a heterogeneous EOS model to simulate the jet flow. We use a stiffened gamma law gas

EOS to model the diesel fuel. We create numerical vapor bubbles directly to replace the mixed liquid–vapor region. The vapor is modeled with a gamma law gas EOS.

2. Numerical modeling

In our present study, the vaporization of the fuel is simulated by the dynamic creation of the vapor bubbles in the fuel. The diesel fuel is treated as a viscous fluid. The thermal conductivity of the fuel is also considered. Because the thermal conductivity and the viscosity are both small, we are able to solve the Navier-Stokes equations with an explicit algorithm. On the liquid/vapor interface boundary, we solve a phase transition problem.

2.1. Dynamic creation of vapor bubbles

We model the vaporization of the fuel with finite sized saturated vapor bubbles. We use circular bubbles with radius $r = 2\Delta x$. Δx is the mesh size. We choose $2\Delta x$ by the numerical experiments. If a bubble evolves to a radius less than $2\Delta x$, it is deleted by the numerical routines. We also define the bubble spacing h as the distance between the centers of two bubbles. When a bubble is first initialized numerically, it should have at least minimum spacing to other bubbles. If the bubble spacing is too small, there will not be enough relaxing time, which results in numerical instability. The typical bubble spacings are $8\Delta x$, $6\Delta x$, $5\Delta x$. In our simulation, we use $8\Delta x$ as the bubble spacing. The vapor is modeled by a gamma law gas EOS.

* Corresponding author. Tel.: +1 (631) 632 8355; Fax: +1 (631) 632 8490; E-mail: glimm@ams.sunysb.edu

We describe our dynamic bubble creation algorithm as follows: For every time step, we check whether in each cell, the liquid pressure p is less than the saturated liquid/vapor pressure P_s calculated by $P_s = P_s(T)$ using the static Clausius-Clapeyron relation. The temperature T is this cell's current temperature. $p < P_s$ indicates the vaporization of the fuel. If there is a 4×4 block of cells that all have $p < P_s$ centered in a larger $(4\Delta x + 2r) \times (4\Delta x + 2r)$ region which is not occupied by the bubbles, we insert a circular bubble in this block. To define the vapor bubble states, we take the average temperature \bar{T} and velocity \bar{U} of the liquid previously defined in these 4×4 cells. Using the static Clausius-Clapeyron relation again, we take the initial vapor pressure to be $P = P_s(\bar{T})$. The vapor density is computed from the EOS. The vapor bubble initial velocity is taken to be \bar{U} .

2.2. Dynamic phase boundaries for compressible fluids

The interface that separates the liquid and the vapor and has a phase transition occurring on it is modeled as a phase boundary.

The phase transition is governed by the compressible Euler equations with heat diffusion,

$$\rho_l + (\rho u)_x = 0 \tag{1}$$

$$(\rho u)_t + (\rho u^2)_x + p_x = 0 \tag{2}$$

$$(\rho E)_t + (\rho E u + p u - \kappa T_x)_x = 0 \tag{3}$$

where $E = 1/2(u^2) + \epsilon$ is the total specific energy, p is the pressure, κ is the thermal conductivity and T is the absolute temperature.

The jump conditions for the dynamic phase boundary are

$$[\rho u] = s[\rho] \tag{4}$$

$$[\rho u^2 + P] = s[\rho u] \tag{5}$$

$$[\rho u E + P u - \kappa T_x] = s[\rho E] \tag{6}$$

where s is the phase boundary moving speed. We use l, v subscripts to represent liquid and vapor respectively. From the Euler equations, we have

$$\rho_v(u_v - s) = \rho_l(u_l - s) \tag{7}$$

$$\rho_v(u_v - s)^2 + p_v = p_l(u_l - s)^2 + p_l \tag{8}$$

$$(\rho_v E_v + p_v)(u_v - s) - \kappa_v T_{v,x} = (\rho_l E_l + p_l)(u_l - s) - \kappa_l T_{l,x} \tag{9}$$

and the change of energy during the phase transition is

$$\epsilon_v + \frac{p_v}{\rho_v} = \epsilon_l + \frac{p_l}{\rho_l} + Q_v \tag{10}$$

where Q_v is the heat of vaporization. We know that on the static phase boundary, the Clausius-Clapeyron

relation holds. For the dynamic phase boundary, we postulate that temperature is continuous but the pressure is not.

We define the mass flux $M = \rho_v(u_v - s) = \rho_l(u_l - s)$. The mass and momentum balance equations give

$$M = -\frac{p_v - p_l}{u_v - u_l} \tag{11}$$

$$M^2 = -\frac{p_v - p_l}{\tau_v - \tau_l}, \tau = \frac{1}{\rho} \tag{12}$$

$$(u_v - s)(u_l - s) = \frac{p_u - p_l}{\rho_v - \rho_l}. \tag{13}$$

Combining with the energy balance equation, we obtain the generalized Hugoniot relation

$$\epsilon_l - \epsilon_v + \frac{p_l + p_v}{2}(\tau_l - \tau_v) = \frac{1}{M}(\kappa_v T_{v,x} - \kappa_l T_{l,x}). \tag{14}$$

If $\kappa_v T_{v,x} \neq \kappa_l T_{l,x}$, a phase transition occurs. We neglect the heat transfer across the shock and rarefaction waves, and account for it only on the phase boundary.

The numerical algorithm for the solutions of dynamical phase transition is described as follows: We assume that we are given the initial values of pressure, density, energy and temperature gradients on both sides of the interface. We first solve a standard Riemann problem for compressible Euler equations without heat conduction. We obtain the interface moving speed s . We assume the equilibrium temperature on the dynamic phase boundary is $\bar{T} = T_l$, where T_l is the liquid temperature from the standard Riemann problem solution, since the liquid has very large heat capacity compared with that of the vapor. We also assume that the vapor states are on the saturated liquid/vapor curve. Then we know the vapor p_v from $p_v = p(\bar{T})$. Using the vapor EOS, the vapor density ρ_v is determined. We now solve Eqs. (14) and (12) with the EOS to get mass flux M and liquid pressure p_l . We compute the liquid/vapor velocity by using the mass balance equation (7):

$$u_l = s + \frac{M}{\rho_l} \tag{15}$$

$$u_v = s + \frac{M}{\rho_v}. \tag{16}$$

We call the above solution the phase boundary solution.

This is a new description for the Riemann problem associated with a phase transition in a fully compressible fluid. We point out that our phase boundary solution is decoupled from acoustic waves. We believe that the 1D phase boundary solution of the full Riemann problem with acoustic waves in general does not exist within the heterogeneous EOS model. In fact our EOS model with a mixed phase region represented by vapor bubbles is inherently 3D where as a Riemann solution is 1D.

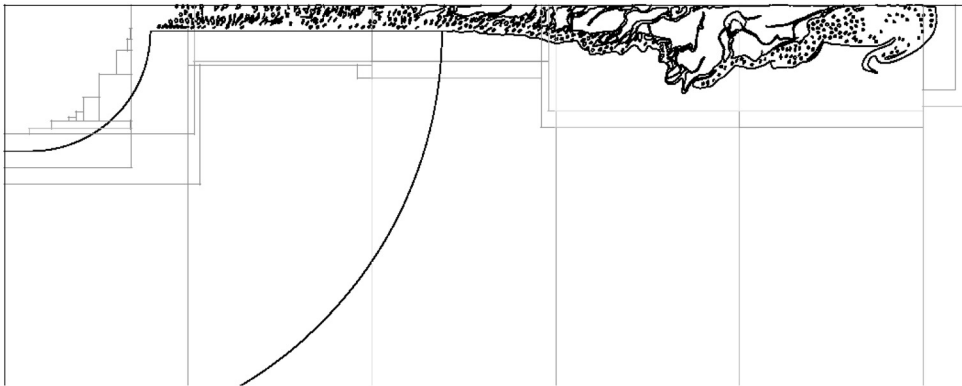


Fig. 1. The plot of the interface and refinement grids.

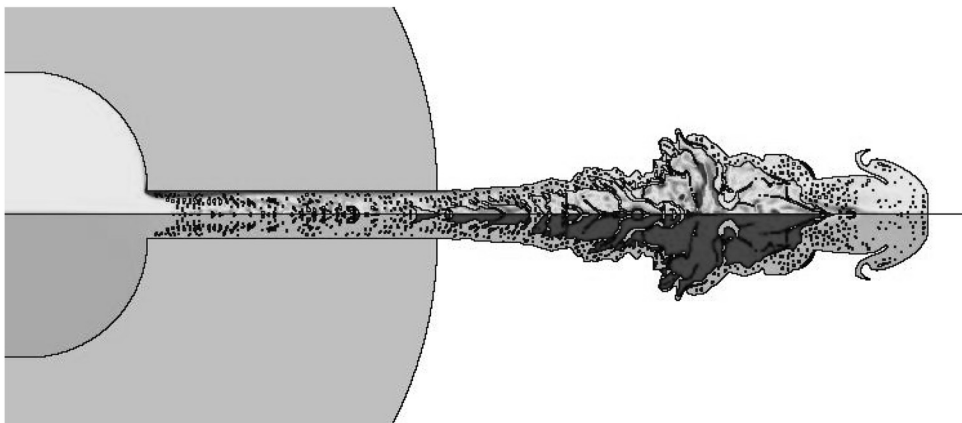


Fig. 2. The plot of vorticity (above) and the density (below).

2.3. Adaptive mesh refinement

The diesel jet flow is multiscale in nature. It requires to resolve various physical patterns such as vortex, shock waves and vacuum. When jet breaks up into droplets and spray (droplets are about 10 microns in size), we need to track these small structures.

We adopted the Burger–Colella [2] adaptive mesh refinement (AMR) to the front tracking method by merging FrontTier with the Overture code, the AMR package developed by the team at Lawrence Livermore National Laboratory. Besides the cells where the estimated errors are larger than the threshold, the cells that contain or are sufficiently close to the interface are also refined. We have solved the dynamic load balancing issue, which must be reconsidered in the context of Front Tracking. We refer to [3] for a detailed description of this work. Figure 1 shows the current simulation with AMR. We use 3 levels of refinement with refinement factor 2. The base level has 170×1000 cells.

3. Simulation results

We have compared our simulation (Fig. 2) with the experimental data [4,5,6,7]. We measured the mass in a 0.55 mm wide observation window centered at 1 mm from the nozzle exit. The mass from our calculation is 20% to 35% higher than the experimental data, (see Fig. 3). We also measured the jet tip velocity. It is 40% to 50% lower than that from the experimental data.

The current conclusion for the bubble insertion is that it improves the mass in the experimental region in comparison with homogeneous EOS. But it seems to slow down the jet tip velocity, and there are still few breakups. We are conducting the mesh refinement studies by using the adaptive mesh refinement in the Front Tracking method [4]. The influences of the other parameters on the spray formation are subjected to further study.

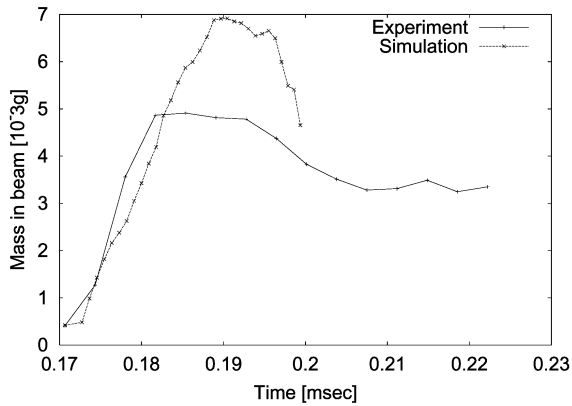


Fig. 3. The plot of mass at 1 mm from the nozzle exit.

References

- [1] Marchese A, Li X, Xu Z, Kim M-N, Samulyak R, Tzanos C, Glimm J, Oh W. Breakup and spray formation in a diesel engine. In: Bathe KJ, editor, Proc of the 2nd MIT Conference on Computational Fluid and Solid Mechanics; Cambridge, MA, 2003.
- [2] Berger M, Colella P. Local adaptive mesh refinement for shock hydrodynamics. *J Comp Phys* 1989;82:64–84.
- [3] Xu Z-L, Glimm J, Li X-L. Front tracking algorithm using adaptively refined meshes. In: Proc of the 2003 Chicago Workshop on Adaptive Mesh Refinement Methods, Chicago, IL, T Plewa, T Linde, VG Weirys, editors, 2004.
- [4] Yue-Y, Poola R, Powel CF, Wang J. Time resolved measurements of supersonic fuel sprays using synchrotron x-rays. *J. Synchrotron Rad* 2000; 7:356–360.
- [5] Tate MW, MacPhee AG, Powell CF. X-ray imaging of shock waves generated by high pressure fuel sprays. *Science* 2002;295:1261–1263.
- [6] Quantitative measurement of a diesel spray core using synchrotron x-ray. In: 8th International Conference on Liquid Atomization and Spray Systems, Pasadena, CA, CF Powel, Y Yue, S Gupta, A McPherson, R Poola, J Wang, editors, 2000.
- [7] Yue-Y, Poola R, Wang J, Lai M, Powel CF, Schaller J. Quantitative x-ray measurements of a diesel spray core. In: Proc of the 14th Annual Conference on Liquid Atomization and Spray Systems (ILASS), Dearborn, MI, 2001.